MICROSILICON LUMINOUS FLUX SWITCH CONTROLLED BY MEANS OF MAGNETIC FIELD

J. Gołębiowski, T. Prohuń
Institute of Theoretical Electrotechnics, Metrology and Materials Science,
Technical University of Łódź, ul.Stefanowskiego 18/22, 90-928 Łódź. POLAND

Keywords: Optical silicon switch, micro-electro-optical-mechanical system (MEOMS), magnetic transducer, FEM.

Abstract: The construction of a silicon beam which is used as a optical switch was presented. The investigated beam consists of three layers: on the silicon base the iron layer is put and it is followed by the aluminium layer. The change of the external magnetic field intensity causes the beam end displacement as well as the change of the luminous flux reflection angle. The influence of the magnetic transducer parameters as well as the field intensity on the luminous flux reflection angle are analysed. The optical system which is steered by the magnetic field was described.

1 THE CONSTRUCTION OF THE OPTICAL SWITCH

Microsilicon structures are commonly applied in the sensors or actuators in which piezoelectric, electrostatic, electromagnetic and magnetic transducers are used (Ciudad, 2004). The scheme of the magnetic transducer with the silicon microbeam is shown in Fig.1.

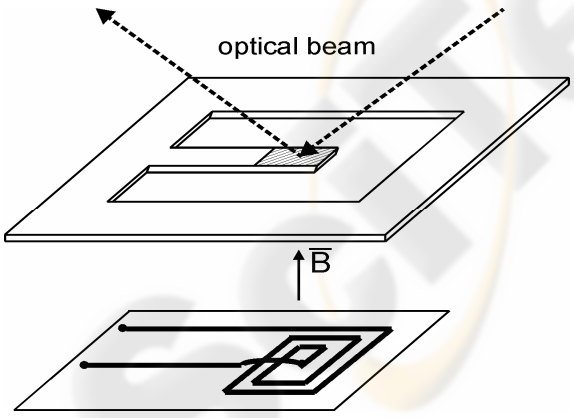

Figure 1: The scheme of the magnetic transducer with the silicon beam

The structure with the micro-mirror on the surface (aluminium layer) can be used to the luminous flux switching in scanners, display units as well as in the optical path switchers for communication (Cho, 2002).

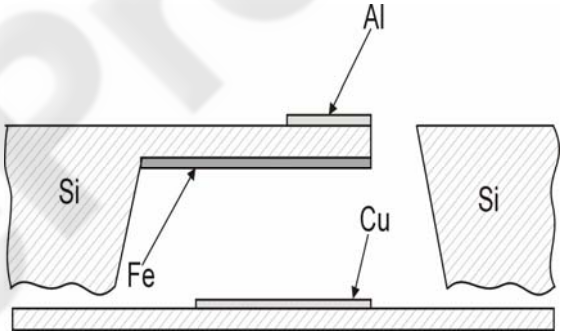

Figure 2: The cross - section of the microstructure with the monocrystalline silicon, Si <100>, base and the magnetic (Fe) and metallic (Al, Cu) layers

The beam structure we studied is shown schematically in Figure 1 and 2 (Wagner, 1992). It consists of a narrow silicon beam (monocrystalline silicon <100>) with of thin magnetic layer (Fe) and metallic layer (mirror- Al). A planar coil was used for the magnetic field generation (Fig.1, Fig.2) (Ripka, 2001).

If a uniform magnetic field is applied to this structure, a pure moment without a translational force is induced. The pure moment or torque generated by the magnetic transducer rotates the beam end through an angle ϕ (Fig.3).

Golebiowski J. and Prohun T. (2005).
MICROSILICON LUMINOUS FLUX SWITCH CONTROLLED BY MEANS OF MAGNETIC FIELD.
In *Proceedings of the Second International Conference on Informatics in Control, Automation and Robotics*, pages 301-306

2 THE ANALYSIS OF THE LUMINOUS FLUX REFLECTION ANGLE IN THE TRANSDUCER CONTROLLED BY MEANS OF THE MAGNETIC FIELD

The beam with the thin ferromagnetic layer is analysed.. It is assumed that the material is isotropic and homogenous as well.

The torque generated under the influence of the external magnetic field can be expressed as (Judy, 1997) :

$$T_{field} = V\left|\vec{M} \times \vec{H}\right| = V \cdot M \cdot H \cdot \sin\alpha \qquad (1)$$

where M is magnetization vector, α is an angle between the magnetization vector and the external field intensity and V is the magnetic material volume.

The magnetic field direction is normal to the normal beam axis as it is shown in Fig. 3.

The torque formed at the external field H causes the magnetization vector M rotation and the rotation angle towards the normal beam axis is equal to β.

When β angle increases the field of the magnetic anisotropy increases as well (Tumanski 1997) according to the equation:

$$H_{anis} = \frac{2 \cdot K}{M_s} \qquad (2)$$

where M_s is the saturation value of the magnetization and K is magnetic anisotropy constant.

The anisotropic field generates the torque T_{anis} which shifts the magnetization vector M towards the beam axis.

The beam is under the influence of the torque of opposite sense $-T_{anis}$. As a results the beam dislocation is observed. For the silicon beam with the ferromagnetic layer and the elasticity coefficient k_{mech} the dislocation generates the mechanic torque which counteracts the magnetic torque $-T_{anis}$ and is equal to:

$$T_{mech} = -k_{mech} \cdot \phi \qquad (3)$$

At the equilibrium state the absolute values of torques are equal.

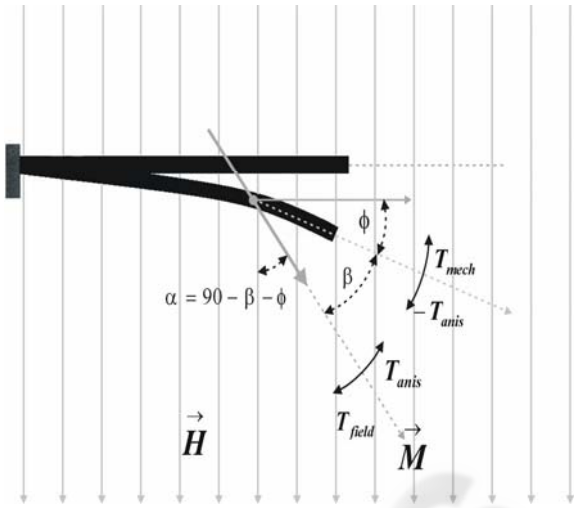

Figure 3: The beam deflection under the influence of the magnetic field H. (Judy, 1996)

The investigated beam consists of three layers: monocrystalline silicon, iron and aluminium.

The analysis is carried out basing on the following assumptions:

For the crystallographic orientation <100> silicon is an orthotropic material with:

Young's modulus $E = 1.31*10^{11}$N/m^2,
Poisson ratio $\nu = 0.0625$,
Density $\rho = 2330$kg/m^3.

The iron layer parameters are equal to:

Young's modulus $E = 2*10^{11}$N/m^2,
Poisson ratio $\nu = 0.29$,
Density $\rho = 7870$kg/m^3.

The aluminium layer parameters are equal to:

Young's modulus $E = 0.7*10^{11}$N/m^2,
Poisson ratio $\nu = 0.33$,
Density $\rho = 2700$kg/m^3.

The model allows to create the dislocation net which reflects the influence of the external magnetic field on the transducer magnetic layer.

At first the density of magnetic energy accumulated in the ferromagnetic layer is calculated. It consists of the external magnetic field energy and the energy of the magnetic anisotropy field. The value of the accumulated energy is used to the determination of the force which influences the beam and causes its displacement.

Regarding the existence of ferromagnetic layer anisotropy the finite element and the coupling field methods as well as FEMLAB program are used in the calculations.

As the FEMLAB programme uses the coupling field method it is possible to take into accounts a variety of physical phenomena and their interactions. The finite element method MES allows to simulate the miscellaneous mechanical structures including

the silicone ones (Lam, 2001). The investigated beam has got an elastic silicon layer and ferromagnetic iron layer.
The analysed structure is divided into 20 000 elements, and the generated net has got 120 000 nodes. The material anisotropy is also taken into considerations.

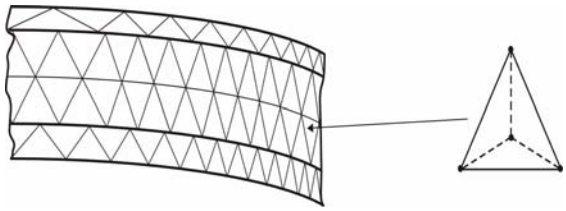

Figure 4: The partition of the structure and an elementary tetrahedron

The elementary tetrahedrons were taken into accounts in the FEMLAB programme calculations (Fig.4). The starting point for the finite element method is a mesh, a partition of the geometry into small units of a simple shape.

In 2D, the method partitions the subdomains into triangles, or mesh elements. The boundaries defined in the geometry are partitioned (approximately) into mesh edges (so-called boundary elements*)* that must conform with the triangles if there is an adjacent subdomain.

In 3D the method partitions subdomains into tetrahedrons. It partitions boundaries in the geometry into triangular boundary elements; and the isolated geometry vertices become mesh vertices (node points*)*.

The size of the elements and their number were selected according to the parted structure size and the assumed boundary conditions.

Then, for the parted structure, the subsequent approximations of the searched variable were made.
The idea is to approximate variable with a function which could describe with a finite number of parameters, the so-called degrees of freedom (DOF). Inserting this approximation into the weak form of the equation generates a system of equations for the degrees of freedom.

3 THE OPTICAL MICROSWITCH SYSTEM

The optical method was applied to measure the placement of the beam end arm. As a light source 2 laser diodes were used. The light ray reflected from the mirror (aluminium layer) incidence on the photodiode.

The change of the beam deflection angle causes the change of the luminous flux reflection angle. The propriety was used in the construction of the luminous flux switch system. The aluminium layer reflect the rays of both laser diodes, but, for the particular beam arm placement, only one of them reflects at the proper angle. Then the ray goes through the apreture and is received by photodiode. The flux from the other laser diode is reflected by the beam mirror and does not fall on the photo detector. The particular beam arm placement allows to receive only one optical flux.

The beam arm placement steering is achieved by the change of the current value in the coil that generates the magnetic field.

The change of the magnetic field induction changes the force which affects the beam arm and the angle of the beam deflection as well.

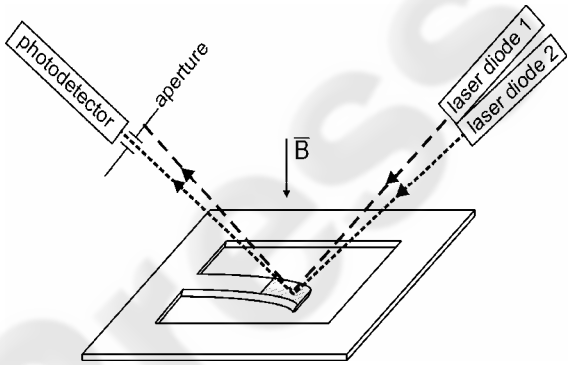

Figure 5: The principle of the optical switch work.

4 RESULTS

The analysis of the beam size influence on the beam end displacement and the angle for the assumed magnetic induction was carried out. According to the technological requirements the maximum allowable beam size changes were assumed and the influence of these parameters on the angle ϕ was analysed.

The analysis of the influence of the beam end parameters on the displacement at the given and equal to B=10mT generated magnetic field induction was carried out. The following model parameters were taken into accounts: the lenght l=5mm, the layer thicknesses 20μm, 10μm and 1μm for the silicon, iron and aluminium layer respectively.

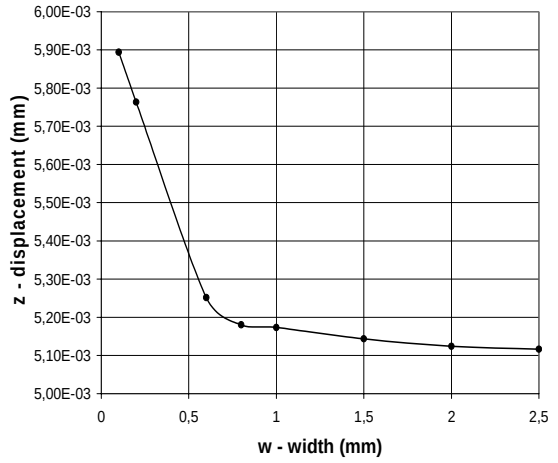

Figure 6: The dependence of the beam end displacement on the beam width w for B=10mT, l= 5mm and d=31μm

For the assumed model the calculations of the influence of the beam width on its displacement were performed. (Fig.6). The beam lenght was l=5mm, and the thicknesses of the layers were 20μm, 10 μm and 1 μm for silicon, iron and aluminium layer respectively.

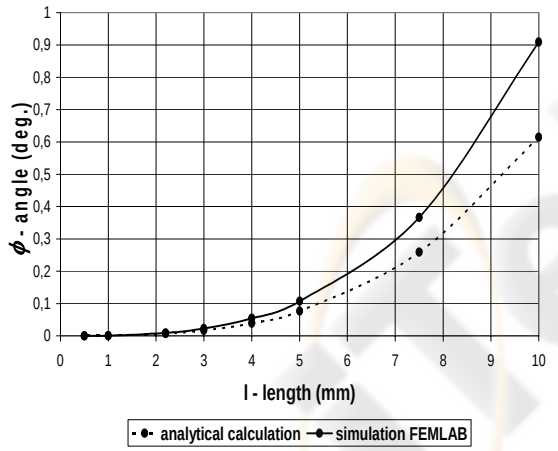

Figure 7: The influence of beam lengths on the angle of its deflection (w=1.5mm, d=31μm, B=10mT).

Fig.7 presents the displacement of the beam end for the different beam lenghts.

According to Judy's (Judy 1996) model the analytical calculations of the beam deflection angle generated by external magnetic field were carried out. The comparison of the calculated results and the data of the FEMLAB program simulation are presented in Fig. 7. As it can be seen the results are in fairly good agreement. The inconsiderable discrepancies are due to the simplifications assumed for the analytical calculations and the material data as well.

In order to maximalize the dislocation the influence of the layer thicknesses was also analysed. In the calculations the following values were applied: l=5mm, w=1.5mm, d_{Si}=20μm, d_{Fe}=10μm, d_{Al}=1μm.

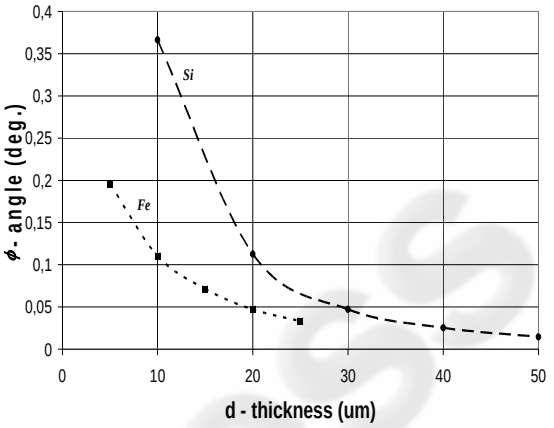

Figure 8: The influence of the layer thickness on the angle of the beam deflection (l=5mm, w=1,5mm, B=10mT).

Fig.8 shows the beam displacement as a function of the thickness of the particular layers.
'Si' characteristic presents the influence of the silicon layer thickness for the assumed thicknesses of the others layers which were equal to d_{Fe}=10μm, d_{Al}=1μm.
'Fe' characteristic presents the dependence of the iron layer thickness for the assumed thicknesses of silicon d_{Si}=20μm and aluminium d_{Al} =1μm layers.
The silicon layer thickness was analyzed in the range of 10μm – 50μm. It is an elastic layer of the base on which transducer was constructed.
The iron layer is a ferromagnetic layer and its thickness can be matched to the field intensity range as well as to the assumed beam displacement.
The aluminium layer is a mirror that is used to measure the beam displacement by means of the optical method. That is why is should be as thin as possible in order not to increase the beam mass.
The influence of the aluminium layer thickness is insignificant and can be omitted.

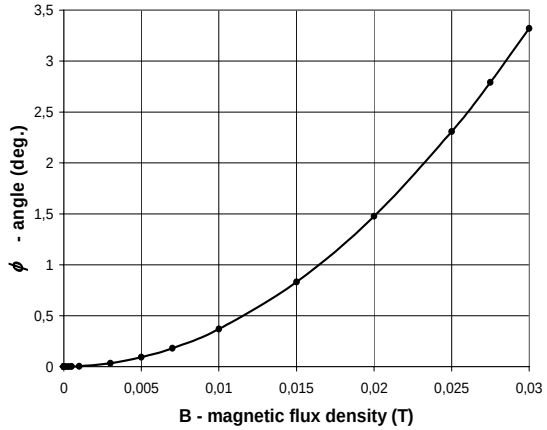

Figure 9: The angular deflection of the beam on magnetic flux density *B*
(*l*=5mm; *w*=0,5mm; d_{Si}=15μm, d_{Fe}=5μm, d_{Al}=1μm)

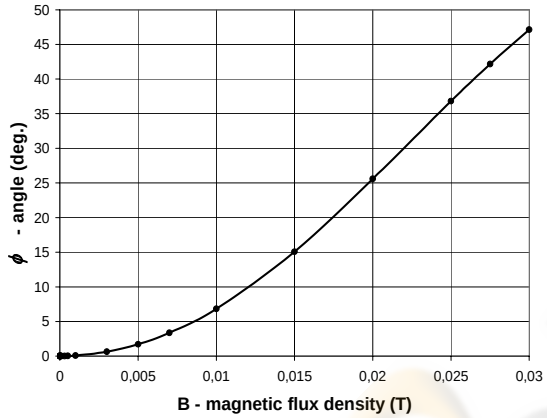

Figure 10: The angular deflection of the beam on magnetic flux density *B*
(*l*=10mm; *w*=1mm; d_{Si}=10μm, d_{Fe}=5μm, d_{Al}=1μm)

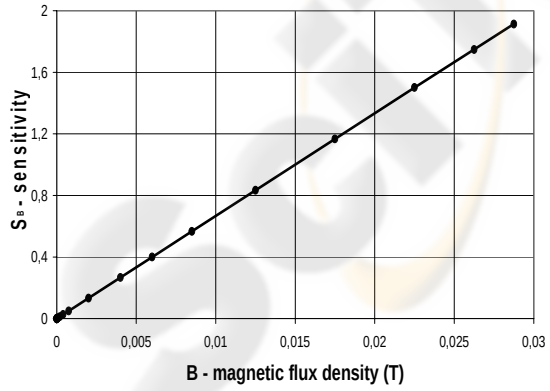

Figure 11: The sensivity coefficient as a function of magnetic flux density *B*
(*l*=5mm; *w*=0,5mm; d_{Si}=15μm, d_{Fe}=5μm, d_{Al}=1μm)

Figs.9 and 10 present the influence of the angular deflection of the beam on the magnetic flux density *B*.

5 CONCLUSIONS

The analysis of the influence of beam size on its displacement leads to the following conclusions:
-The maximum sensitivity coefficient S_w=0.0125deg./mm ($S_w=\Delta\phi/\Delta w$) was observed for the beam width in the range 0.1mm – 0.6mm, (for *l*=5mm, *d*=31μm, *B*=10mT),
-The maximum sensitivity coefficient S_l=0.217deg./mm ($S_l=\Delta\phi/\Delta l$) was obtained for the beam length in the range of 7,5mm – 10mm, (for *w*=1.5mm, *d*=31μm and *B*=10mT).
According to the expectations the maximum displacements were obtained for the beams with the maximum length (10mm) and minimum width (0.1mm).
The analysis of the influence of the particular layer thickness on the sensitivity coefficients leads to the following statements:
-The maximum sensitivity coefficient S_{dSi}=0.0254deg./μm was observed for the silicon layer thickness in the range of 10μm – 20μm,
-The maximum sensitivity coefficient S_{dFe}=0.0171deg./μm was obtained for the thickness in the range of 5μm – 10μm.
The aluminium layer is a mirror and its thickness is a requisite of the technological conditions. The most commonly the aluminium layer thickness is in the range of 0.5μm – 1μm. The layer only slightly influences the beam displacement.
The function of the angle changes depending on the magnetic field induction values is shown in Fig.9.
The change of the external magnetic field induction in the range of 100μT – 30mT causes the displacement change from 1.7nm to 0.156mm. The maximum sensitivity coefficient s_B=1.67 ($s_b=(\Delta\phi/\phi)/(\Delta B/B)$) was obtained for induction in the range 20mT – 30mT, whereas for the range of 100μT – 1mT the coefficient is equal to s_B=0.037.
For the generated field induction *B*=30mT the beam displacement equal to 3.30 deg. was achieved.
The usage of the presented beam as a steering element needs to acquire the beam deflection angle as high as possible. It can be carried into effect by beam elongation. (Fig.10. The beam lenght is equal to *l*=10mm, its width *w*=1mm and its thickness *d*=16μm, *B*=30mT, ϕ=47deg.). The beam deflection angle can also be maximalized by narrowing of the beam fore - part and by enlarging of the magnetic material mass (which is used only in the beam end - part).

REFERENCES

Ahn C. H., Kim Y. J., Allen M. G., 1993. *A planar variable reluctance magnetic micromotor with fully integrated stator and wrapped coils.* Proceedings of IEEE Micro Electro Mechanical Systems (MEMS '93), pp. 1-6.

Bosch D., Heimhofer B., Muck G., Seidel H., Thumser U., and Welser W., 1993. *A silicon microvalve with combined electromagnetic/electrostatic actuation.* Sensors and Actuators A, v. A37-A38, pp. 684-692.

Cho H.J., Ahn C.H., 2002. *A bidirectional magnetic microactuator using electroplated permanent magntet arrays. J.*, Microelectromech. Syst. 11, pp. 78-84.

Ciudad D., Aroca C., Sanchez M.C., Lopez E., Sanchez P., 2004. *Modelling and fabrication of a MEMS magnetostatic magnetic sensor.* Elsevier Sensors and Actuators, A 115, pp. 408-416.

Cullity B.D., 1972. *Introduction to magnetic Materials*. MA: Addison-Wesley, p. 527.

Gołębiowski J., Prohuń T., Rybak M., 2004. *Modelling of the Silicon Membrane Vibrations Generated by Means of Electromagnetic Forces*. WSEAS Transaction on Systems, Issue 7, vol.3, pp.2538-2540.

Gołębiowski J., 2001. *Modelling of measurement microsystems with membranes of silicone ultrasonic sensors.* Proc. of 2001 WSES/IEEE Intern. Conference on Simulation S IM'01/IEEE, Malta, pp.87-90.

Guckel H., Christenson T. R., Skrobis H. J., Jung T. S., Klein J., Hartojo K. V, Widjaja I., 1993. *A first functional current excited planar rotational magnetic micromotor.* Proceedings of IEEE Micro Electro Mechanical Systems (MEMS '93), pp. 1-6.

Irons H.R. Schwee L.J., 1972. *Magnetic thin-film magnetometers for magnetic field measurement.* IEEE Trans. Magn. Vol. 8, pp. 61-65.

Judy J.W., Muller R.S., 1996. *Magnetic Microactuation of Torsional Polysilicon Structures.* Sensors and Actuators A, v. A53, no. 1-3, pp. 392-397.

Judy J.W., Muller R.S., 1996. *Batch-Fabricated, Addressable, Magnetically Actuated Microstructures.* Tech. Dig. Solid-State Sensor and Actuator Workshop, pp. 187-190.

Judy J.W., Muller R.S., 1997. *Magnetically Actuated, Addressable Microstructures.* Journal of Microelectromechanical Systems, vol. 6, no. 3, pp. 249-256.

Konno H., 1991. *Integrated ferromagnetic MR sensors.* J. Appl. Phys., vol. 69, pp 5933-5935.

Lachowicz H., 1995. *Nowe materiały i zjawiska magnetyczne*. Elektronika, vol. 36, pp. 12-17.

Lam T., Darling R.B., 2001. *Psychical Modelling of MEMS Cantilever Beams and the Measurement of Stiction Force, Modelling and Simulation of Microsystems.* ISBN 0-9708275-0-4, pp. 418-421.

Liao S., 1990. *Electrodeposition of magnetic materials for thin-film heads*. IEEE Transactions on Magnetics, vol. 26 no.1 pp. 328-332.

Ripka P., 2001. *Magnetic Sensors and Magnetometers.* Artech House Inc., pp. 381-382.

Roark R.J., 1989. *Roark's Formulas for Stress and Strain*. 6th Edition, Warren C. Young Editor, New York, McGraw-Hill Book Co.

Tang W C., Nguyen T.-C.H., Judy M. W., Howe R. T., 1990. *Electrostatic-comb drive of lateral polysilicon resonators.* Sensors and Actuators A, v. A21, no. 1-3, pp. 328-331.

Timoshenko S.P., Goodier J.N., 1970. *Theory of Elasticity.* 3rd Edition, New York, McGraw-Hill Book Co.

Tumański S., 1997. *Cienkowarstwowe czujniki magnetorezystancyjne*. Oficyna Wydawnicza Politechniki Warszawskiej.

Tumański S. 1985. *Współczesne metody pomiaru słabych pól magnetycznych*. Prace Naukowe Politechniki Świętokrzyskiej, vol. 16, pp. 81-95.

Wagner B., Benecke W., Engelmann G., Simon I., 1992. *Microactuators with moving magnets for linear, torsial, or multiaxial motion*. Sensors and Actuators A (Physical), v. A32, no. 1-3, pp. 598-603.